

Broadening of optical transitions in polycrystalline CdS and CdTe thin films

Jian Li, Jie Chen, and R. W. Collins

Citation: *Appl. Phys. Lett.* **97**, 181909 (2010); doi: 10.1063/1.3511744

View online: <http://dx.doi.org/10.1063/1.3511744>

View Table of Contents: <http://apl.aip.org/resource/1/APPLAB/v97/i18>

Published by the [American Institute of Physics](#).

Related Articles

CdS nanofilms: Effect of film thickness on morphology and optical band gap

J. Appl. Phys. **112**, 123512 (2012)

Effect of betanin natural dye extracted from red beet root on the non linear optical properties ZnO nanoplates embedded in polymeric matrices

J. Appl. Phys. **112**, 123104 (2012)

Response to "Comment on 'Room temperature photoluminescence from ZnO quantum wells grown on (0001) sapphire using buffer assisted pulsed laser deposition'" [*Appl. Phys. Lett.* **101**, 256101 (2012)]

Appl. Phys. Lett. **101**, 256102 (2012)

Temperature-dependent photoluminescence of ZnO films codoped with tellurium and nitrogen

J. Appl. Phys. **112**, 103534 (2012)

Quadrupole effects in photoabsorption in ZnO quantum dots

J. Appl. Phys. **112**, 104323 (2012)

Additional information on *Appl. Phys. Lett.*

Journal Homepage: <http://apl.aip.org/>

Journal Information: http://apl.aip.org/about/about_the_journal

Top downloads: http://apl.aip.org/features/most_downloaded

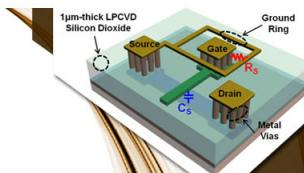
Information for Authors: <http://apl.aip.org/authors>

ADVERTISEMENT



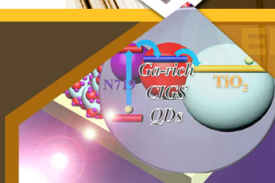
**EXPLORE WHAT'S
NEW IN APL**

SUBMIT YOUR PAPER NOW!



SURFACES AND INTERFACES

Focusing on physical, chemical, biological, structural, optical, magnetic and electrical properties of surfaces and interfaces, and more...



ENERGY CONVERSION AND STORAGE

Focusing on all aspects of static and dynamic energy conversion, energy storage, photovoltaics, solar fuels, batteries, capacitors, thermoelectrics, and more...

Broadening of optical transitions in polycrystalline CdS and CdTe thin films

Jian Li, Jie Chen, and R. W. Collins^{a)}

Department of Physics and Astronomy, University of Toledo, Toledo, Ohio 43606, USA

(Received 15 September 2010; accepted 12 October 2010; published online 3 November 2010)

The dielectric functions ε of polycrystalline CdS and CdTe thin films sputter deposited onto Si wafers were measured from 0.75 to 6.5 eV by *in situ* spectroscopic ellipsometry. Differences in ε due to processing variations are well understood using an excited carrier scattering model. For each sample, a carrier mean free path λ is defined that is found to be inversely proportional to the broadening of each of the band structure critical points (CPs) deduced from ε . The rate at which broadening occurs with λ^{-1} is different for each CP, enabling a carrier group speed v_g to be identified for the CP. With the database for v_g , ε can be analyzed to evaluate the quality of materials used in CdS/CdTe photovoltaic heterojunctions. © 2010 American Institute of Physics. [doi:10.1063/1.3511744]

Heterojunctions of thin film polycrystalline CdS and CdTe have attracted increasing attention for applications in low cost photovoltaic (PV) modules in the glass superstrate configuration.¹ A major challenge in the PV applications of polycrystalline films arises from the variation in materials structure that leads to variations in optical and electronic properties critical for device optimization. Spectroscopic ellipsometry (SE) has been used extensively to study the optical properties of polycrystalline semiconductors for comparison with their single crystal counterparts. Early SE studies accounted for the significant broadening of the critical point (CP) features in the dielectric functions ε of polycrystalline Si films through an effective medium theory assuming a microscopic mixture of crystalline, amorphous, and void components.² Subsequent studies attributed the CP broadening in polycrystalline Si and Ge films to the role of grain boundaries and defects, rather than to a well-defined amorphous phase.³ Later, the CP broadening in GaAs, ion bombarded to generate defects, was consistently quantified using a concept of excited carrier scattering by defects.⁴

In this study, two series of polycrystalline CdS and CdTe thin films were magnetron sputtered onto native oxide covered crystalline Si (c-Si) wafers using the processing parameters of Table I. The key parameter is substrate temperature T , as determined from a calibration based on an *in situ* SE measurement of the c-Si ε spectra prior to each deposition.⁵ Each film was grown to a thickness of 500–1000 Å and then cooled from T to 15 °C under vacuum for SE measurement. Such a thickness was selected to reduce the effect of inhomogeneities versus depth observed in thick films.⁶ In addition, as shown in Table I, a $T=188$ °C CdTe sample was measured after a 5 min postdeposition anneal at 387 °C in CdCl₂ vapor and dry air, a processing step well-documented to enhance PV device performance.¹

A rotating compensator multichannel ellipsometer^{7,8} (J.A. Woollam Co. M-2000) was used in this study to measure the angles (ψ, Δ) from 0.75 to 6.5 eV, where $\tan \psi \exp(i\Delta) \equiv r_p/r_s$. Here r_p and r_s are the complex amplitude reflection coefficients for p and s polarized light. During film deposition, (ψ, Δ) spectra were acquired in 1–3 s, as averages over ~30–90 compensator optical cycle pairs. The

bulk layer thickness d_b and the surface roughness thickness d_s were accurately determined from the real time (ψ, Δ) spectra by combining inversion and least-squares regression.⁹ Assuming that these values do not change upon cooling to 15 °C, $\varepsilon = \varepsilon_1 + i\varepsilon_2$ of each film is obtained by inversion of (ψ, Δ) at 15 °C.

Figure 1(a) shows the 15 °C spectra in ε for two CdS films with the indicated T values. Three distinct CPs are evident and denoted as E_0 , E_1 -A, and E_1 -B.¹⁰ Figure 1(b) compares the 15 °C spectra in ε for the CdTe film deposited at $T=188$ °C with results for single crystal CdTe.¹¹ Four CPs are evident for CdTe and denoted as E_0 , E_1 , $E_1 + \Delta_1$, and E_2 .¹² Differences in the CP feature widths can be observed in Fig. 1 (see insets). To quantify these differences, the second derivatives $d^2\varepsilon/dE^2$ were fit based on the equation

$$\varepsilon = \sum_n A_n [\exp(i\phi_n)] [E_n - E - i(\Gamma_n/2)]^{\mu_n}, \quad (1)$$

assuming parabolic bands and Lorentzian broadening.¹³ In Eq. (1), E is photon energy; A_n , E_n , Γ_n , μ_n , and ϕ_n are the amplitude, band gap, broadening parameter, exponent, and phase of the n th CP, respectively.

Second derivative spectra for polycrystalline CdS and CdTe are shown in Fig. 2 including data and fits, the latter using the expression of Eq. (1). The best fit Γ_{E_0} of CdS and $\Gamma_{E_1 + \Delta_1}$ of CdTe are plotted versus deposition temperature T in Fig. 3(a). Also shown are the results for the CdTe sample treated with CdCl₂ at 387 °C. Among the CdS films, the one deposited at $T=310$ °C has the smallest broadening parameter for each of the E_0 , E_1 -A, and E_1 -B CPs. In fact, the CP features in ε for this sample are even sharper than those reported for single crystal CdS.¹⁴ This is likely due to near-

TABLE I. Processing parameters used in this study. (sccm denotes cubic centimeter per minute at STP).

Deposited material	rf power (W)	Ar pressure (mTorr)	Ar flow (sccm)	Deposition/(CdCl ₂ treated) temperature (°C)
CdS	50	10	23	145–320
CdTe	60	18	23	188–304 387 (CdCl ₂)

^{a)}Electronic mail: robert.collins@utoledo.edu.

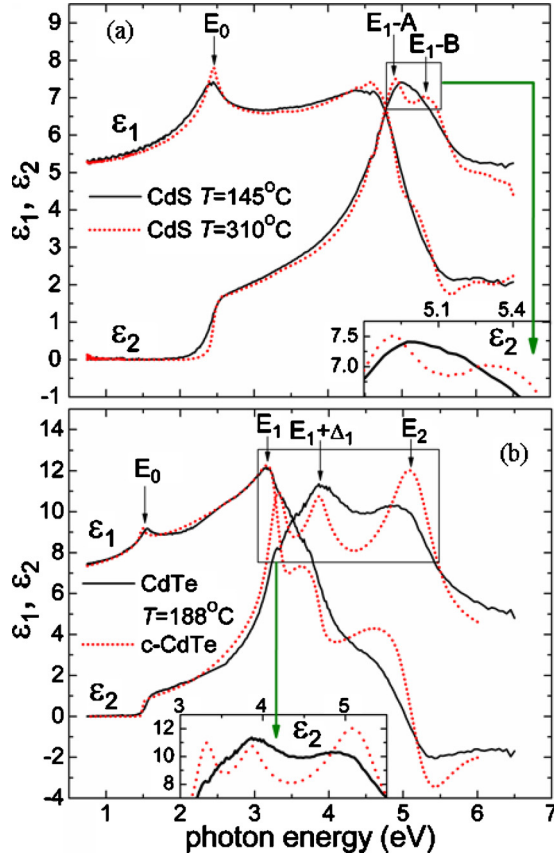


FIG. 1. (Color online) The 15°C complex dielectric functions $\epsilon = \epsilon_1 + i\epsilon_2$ of (a) two CdS films with indicated T values, and (b) the $T = 188^\circ\text{C}$ CdTe film along with single crystal CdTe. The major CPs are marked.

surface polishing damage in the crystal. Thus, Γ_n for the $T = 310^\circ\text{C}$ sample can be taken to approximate that of single crystal CdS (denoted by Γ_{bn} ; b : bulk).

The broadening parameter Γ_{b,E_0} for the fundamental band gap describes how far in k -space from the zone center an excitation can occur while contributing to CP transitions. The dominant group speed $v_{g,E_0} = dE/d(\hbar k)|_{k=k_v}$ of a carrier can be estimated to occur at the energy $E_v = \hbar^2 k_v^2 / 2\mu^* = \Gamma_{b,E_0} / 2$, above or below the CP where $(\mu^*)^{-1} = (m_e^*)^{-1} + (m_h^*)^{-1}$ is the reduced effective mass and \hbar is Planck's constant. The result for electrons is

$$v_{g,E_0} = \{\Gamma_{b,E_0} m_h^* / [m_e^* (m_e^* + m_h^*)]\}^{1/2}. \quad (2)$$

With $m_e^* \approx 0.2m$ and $m_h^* \approx 0.7m$ as the electron and hole effective masses for CdS, where m is the electron mass,¹⁵ v_{g,E_0} is found to be $\sim 2.2 \times 10^5$ m/s. The result for holes is 3.5 times lower and so hole scattering is less likely to contribute.

If the broadening effect is due to a limited excitation lifetime due to scattering of carriers, then

$$\Gamma_n = \Gamma_{bn} + (\hbar v_{gn} / \lambda), \quad (3)$$

where v_{gn} is the dominant group speed associated with the n th CP and λ is a mean free path.⁴ If scattering occurs due to grain boundaries in the polycrystalline films, then λ is monotonically related to R , the grain radius. Using the values of v_{g,E_0} and Γ_{b,E_0} for single crystal CdS and applying Eq. (3), λ can be calculated versus T as shown in Fig. 3(b). Uncertainties in v_{g,E_0} and Γ_{b,E_0} influence the magnitude of λ but not

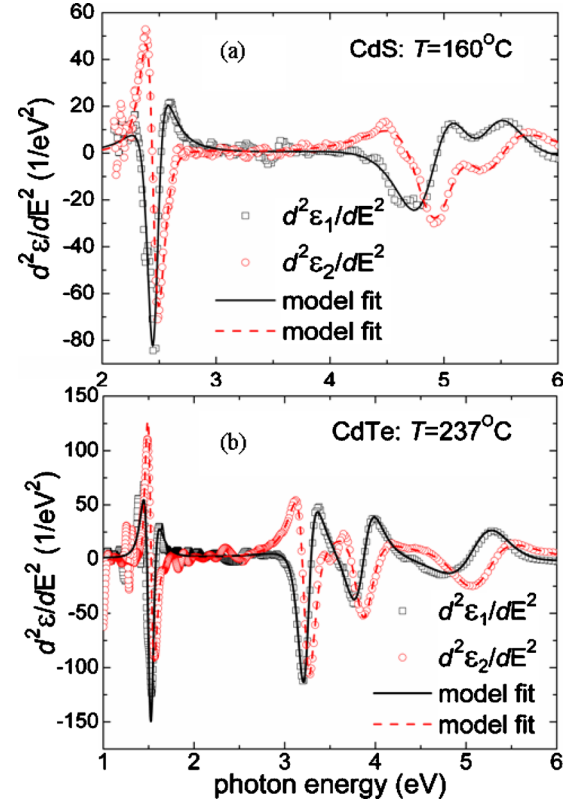


FIG. 2. (Color online) The second derivative spectra of 15°C complex dielectric functions ϵ of (a) the CdS film deposited at $T = 160^\circ\text{C}$, and (b) the CdTe film deposited at $T = 237^\circ\text{C}$. The fits are based on Eq. (1).

the sample-dependent trend. It can be seen that an increase in T from 150 to 300°C for sputtered CdS films leads to an increase in λ by a factor of 30, and by inference a strong increase in grain size, also corroborated by atomic force microscopy images. As a check of the validity of the approach, the widths Γ_{E_1-A} and Γ_{E_1-B} for CdS are plotted versus λ^{-1} in

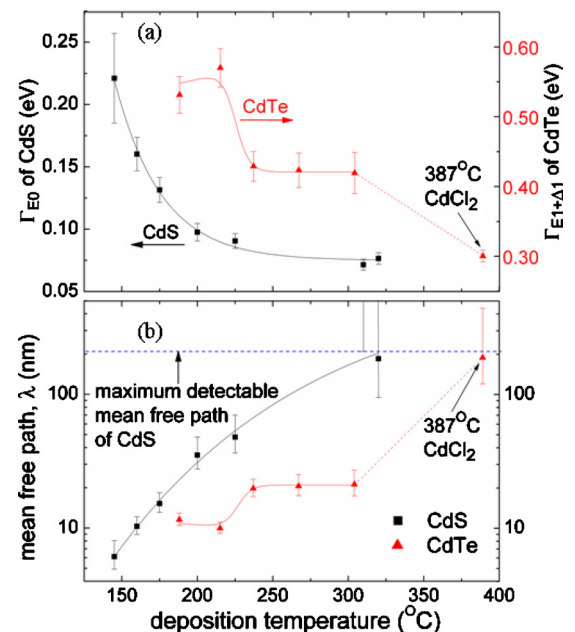


FIG. 3. (Color online) Plotted as functions of deposition temperature include: (a) the broadening parameters used to deduce mean free path in polycrystalline CdS and CdTe films; and (b) mean free path results deduced from Eq. (3).

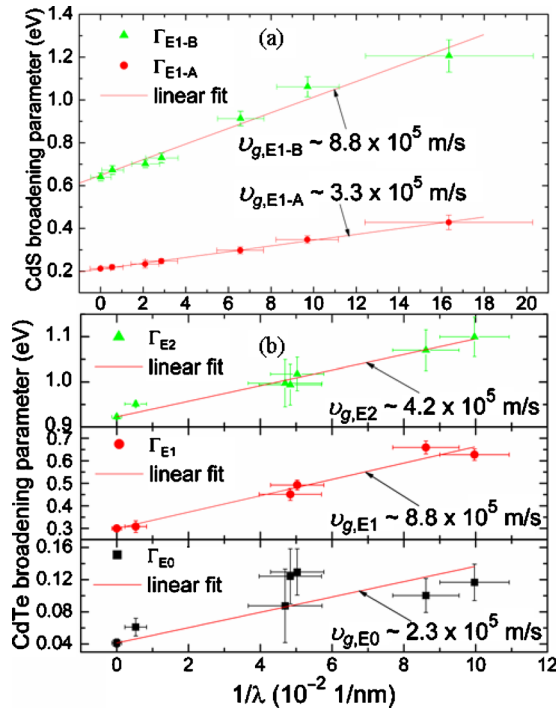


FIG. 4. (Color online) The broadening parameters plotted as functions of the reciprocal of deduced mean free path for (a) CdS and (b) CdTe. The group speeds of excited carriers are calculated from the slopes of the linear fits using Eq. (3).

Fig. 4(a). The linear relations predicted by Eq. (3) are closely followed yielding group speeds for E_1 -A and E_1 -B of 3.3×10^5 m/s and 8.8×10^5 m/s, respectively.

A similar procedure has been performed for extracting the sample λ values and the CP v_{gn} values for the series of CdTe films prepared at different T . In this case, the CdTe E_0 transition has weaker amplitude than that of CdS as shown in Fig. 1. As a result, the Γ_{E0} values are more difficult to determine accurately compared to those of CdS. To generate more accurate λ values, the strong $E_1 + \Delta_1$ transition is used instead of E_0 ; see Fig. 1(b). The band structure associated with the $E_1 + \Delta_1$ transition is not well-known, however, and thus $v_{g,E1+\Delta_1}$ is not known in advance. In this case, $v_{g,E1+\Delta_1}$ is determined iteratively as 6.9×10^5 m/s, which then ensures that $v_{g,E0} = 2.3 \times 10^5$ m/s, as estimated using $m_e^* \approx 0.11m$ and $m_h^* \approx 0.4m$ for CdTe.^{15,16}

The CdTe λ values shown in Fig. 3(b) reveal a weaker variation with T than that for CdS. The step increase in λ near $T = 225$ °C accompanies a well characterized stress-induced structural transition⁶ versus T at a given d_b that leads to an increase in grain size. A very important result however, is the large increase in λ generated by the CdCl₂ treatment,

indicating a significant grain size increase. The relationships that establish the group speeds for different CPs in CdTe are shown in Fig. 4(b) and lead to the values of $v_{g,E1} = 8.8 \times 10^5$ m/s and $v_{g,E2} = 4.2 \times 10^5$ m/s. The poorer fit for E_0 among all the results in Fig. 4 is attributed to its weak amplitude as well as to the averaging that occurs with depth in conjunction with inhomogeneity. This is also observed for the E_1 transition of the $T = 304$ °C sample, leading to exclusion of this result from Fig. 4.

In summary, the dielectric functions of polycrystalline CdS and CdTe films have been determined using *in situ* SE. The widths of all three CPs in CdS and all four CPs in CdTe can be predicted on the basis of a single sample-dependent mean free path parameter, using the group speed associated with each of the CPs determined here. This database enables SE to be used *ex situ* for quality evaluation of materials in CdS/CdTe heterojunction solar cells.

This research was supported by DOE Grant No. DE-FG36-08GO18067 and by the State of Ohio Third Frontier's Wright Centers of Innovation Program.

¹B. E. McCandless and J. R. Sites, in *Handbook of Photovoltaic Science and Engineering*, edited by A. Luque and S. Hegedus (Wiley, New York, 2003), p. 617.

²D. E. Aspnes, *Thin Solid Films* **89**, 249 (1982).

³R. W. Collins, H. Windischmann, J. M. Cavese, and J. Gonzalez-Hernandez, *J. Appl. Phys.* **58**, 954 (1985).

⁴G. F. Feng and R. Zallen, *Phys. Rev. B* **40**, 1064 (1989).

⁵P. Lautenschlager, M. Garriga, L. Vina, and M. Cardona, *Phys. Rev. B* **36**, 4821 (1987).

⁶J. Li, J. Chen, N. J. Podraza, and R. W. Collins, *Proceedings of the Fourth World Conference on Photovoltaic Energy Conversion* (IEEE, Piscataway, NJ, 2006) p. 392.

⁷J. Lee, P. I. Rovira, I. An, and R. W. Collins, *Rev. Sci. Instrum.* **69**, 1800 (1998).

⁸B. Johs, J. Hale, N. J. Ianno, C. M. Herzinger, T. Tiwald, and J. A. Woollam, in *Optical Metrology Roadmap for the Semiconductor, Optical, and Data Storage Industries II*, edited by A. Duparre and B. Singh (SPIE, Bellingham, WA, 2001), Vol. 4449, p. 41.

⁹I. An, Y. M. Li, H. V. Nguyen, and R. W. Collins, *Appl. Phys. Lett.* **59**, 2543 (1991).

¹⁰P. Hofmann, K. Horn, A. M. Bradshaw, R. L. Johnson, D. Fuchs, and M. Cardona, *Phys. Rev. B* **47**, 1639 (1993).

¹¹B. Johs, C. M. Herzinger, J. H. Dinan, A. Cornfeld, and J. D. Benson, *Thin Solid Films* **313-314**, 137 (1998).

¹²C. C. Kim, M. Daraselia, J. W. Garland, and S. Sivanathan, *Phys. Rev. B* **56**, 4786 (1997).

¹³R. W. Collins and A. Ferlauto, in *Handbook of Ellipsometry*, edited by H. G. Tompkins and E. A. Irene (William Andrew, Norwich, NY, 2005), p. 150.

¹⁴S. Ninomiya and S. Adachi, *J. Appl. Phys.* **78**, 1183 (1995).

¹⁵D. T. F. Marple, *Phys. Rev.* **129**, 2466 (1963).

¹⁶J. I. Pankove, *Optical Processes in Semiconductors* (Dover, New York, 1975), p. 412.